Published in final edited form as:
Eur J Oral Sci. 2012 June ; 120(3): 185–194. doi:10.1111/j.1600-0722.2012.954.x.

Titanium alloy surface oxide modulates the conformation of adsorbed fibronectin to enhance its binding to $\alpha_5\beta_1$ integrins in osteoblasts

Bruce E. Rapuano[a], **Jani Jae Eun Lee**[a], and **Daniel E. MacDonald**[a,b,c,*]

[a]Hospital for Special Surgery affiliated with the Weill Medical College of Cornell University, 535 East 70th Street, New York, NY 10021, USA

[b]General Medical Research, James J. Peters VA Medical Center, 130 West Kingsbridge Road, Bronx, NY, 10468, USA

[c]Langmuir Center for Colloids and Interfaces, Columbia University, 911 S.W. Mudd Building, Mail Code 4711, 500 West 120th Street, New York, NY, 10027, USA

Abstract

Our laboratory has previously demonstrated that heat (600 °C) or radiofrequency plasma glow discharge (RFGD) pretreatment of a titanium alloy (Ti6Al4V) increases the net-negative charge of the alloy's surface oxide and the attachment of osteoblastic cells to adsorbed fibronectin. The purpose of the current study was to investigate the biological mechanism by which these surface pretreatments enhance the capacity of fibronectin to stimulate osteoblastic cell attachment. Each pretreatment was found to increase the binding (measured by ELISA) of a monoclonal anti-fibronectin Ig to the central integrin-binding domain of adsorbed fibronectin, and to increase the antibody's inhibition of osteogenic cell attachment (measured using the hexosaminidase assay). Pretreatments also increased the binding (measured by ELISA) of anti-integrin Igs to the α_5 and β_1 integrin subunits that became attached to fibronectin during cell incubation. These findings suggest that negatively charged surface oxides of Ti6Al4V cause conformational changes in fibronectin that increase the availability of its integrin-binding domain to $\alpha_5\beta_1$ integrins.

Keywords

fibronectin; conformation; osteoblast; integrins; titanium alloy

Although the outcomes of orthopaedic and dental implant procedures are usually successful, in many instances the long-term stability and functionality of the implant cannot be achieved. Implant loosening and failure is still a significant problem with a sizeable percentage of hip arthroplasties. In fact, 25% of hip-replacement procedures are revisions for previous implant failure (1). Despite the reported long-term predictability of dental implants (2,3), failures do occur in 10% of cases within a 5-year period (4). The quality and quantity of bone that forms at the implant–skeletal interface is generally believed to be one of the major determinants for implant success (5). Therefore, improving fixation by

*To whom reprint requests should be sent: Daniel E. MacDonald, Hospital for Special Surgery, 535 East 70th Street, New York, NY 10021, USA. Telefax: +1–212–7747877, dem14@columbia.edu.

Conflict of Interest

The authors do not have a financial relationship with the organization that sponsored the research. The authors declare that they have no conflict of interest.

enhancing the attachment and function of osteoblastic cells at the implant surface is likely to decrease substantially the likelihood of implant failure.

Commercially pure titanium (cpTi) and its alloy [titanium-6/aluminum-4/vanadium (Ti6Al4V)] are commonly used as implantable materials. Commercially pure titanium is used in dentistry and in maxillofacial reconstruction (6). The Ti6Al4V alloy exhibits superior strength and a lower modulus of elasticity that, coupled with its excellent biocompatibility, make it a favoured material for orthopaedic applications (7). The Ti6Al4V alloy has also been successfully utilized in the dental field (8). Both titanium and its alloys form an active oxide layer that readily interacts with cell-surface proteins and with extracellular matrix proteins produced by cells. It is this superficial oxide found on both metals, TiO_2 being the most abundant, that provides a biocompatible interface with peri-implant tissues (7,9). Altering the surface of titanium-implant materials has been shown to affect protein adsorption, cell–substrate interactions, and tissue development (10). However, the mechanisms by which surface oxide properties modulate the bioactivity of bound osteogenic proteins to influence osseointegration are poorly understood.

Proteins of the extracellular matrix, which function, in part, as sites of attachment for osteoblasts in skeletal tissues (11), have been tested as implant surface coatings to facilitate osteoblast attachment and to promote osseointegration. Our laboratory and others have studied extracellular matrix proteins such as fibronectin or human bone sialoprotein (hBSP), or hBSP peptides, following their non-covalent adsorption (12–16) or covalent grafting (17–20) to the implant surface oxide to increase surface coverage by osteoblasts.

Cell adhesion to fibronectin and to other matrix proteins is primarily mediated by integrin receptors that recognize the tripeptide arginine-glycine-aspartic acid (RGD) as an important protein-binding site (20). However, when fibronectin is adsorbed to an implant surface, it is not known to what degree binding sites in the protein are available for interactions with integrin receptors or how the integrin-binding activity of fibronectin might be influenced by the properties of the surface oxide.

Our laboratory has demonstrated that pretreating the Ti6Al4V surface oxide with heat (600 °C) or radiofrequency plasma glow discharge (RFGD) dramatically increases the number of osteoblastic cells that attach to adsorbed fibronectin (21,22). We have also shown that the pretreatment of the titanium alloy, Ti6Al4V, with heat or RFGD increases the surface oxide's negative net charge (23). Other studies have found that fibronectin adsorbed to negatively charged surfaces exhibits a more extended or relaxed conformation (24–26) and a higher cell-attachment activity (26–28) compared with less-charged surfaces. These findings suggest that substrates with negatively charged functional groups can increase the functional presentation of the integrin-binding domain of fibronectin by inducing conformational changes in the protein upon its adsorption. Such structural changes in the adsorbed protein would hypothetically promote cell attachment by increasing the binding of fibronectin to integrin receptors. Our earlier studies (21,22) did not directly measure the effects of surface pretreatments of Ti6Al4V on fibronectin conformation or the binding of the adsorbed protein to specific integrin receptors. Therefore, in the current study we endeavoured to clarify the biological mechanism for the effects of pretreatment with heat or with RFGD on osteoblastic cell-attachment activity to fibronectin. To achieve this goal, we tested the hypothesis that these pretreatments increase the exposure of the fibronectin integrin-binding domain and its availability to form complexes with integrin receptors, putatively through protein-conformational changes.

Material and Methods

Materials

Fetal bovine serum (FBS), PBS, Dulbecco's PBS (DPBS) and cell culture media were from Invitrogen (Carlsbad, CA, USA). BSA (Fraction V; essentially fatty acid-free) and human plasma fibronectin were purchased from Sigma-Aldrich (St Louis, MO, USA). The cross-linker 3,3′-dithiobis(sulfosuccinimidyl propionate) (DTSSP) was acquired from Pierce Chemical (Rockford, IL, USA). The monoclonal anti-fibronectin Ig, IST-4, was obtained from Sigma-Aldrich. The monoclonal anti-fibronectin Ig, HFN7.1, was obtained from the Developmental Studies Hybridoma Bank (Iowa City, IA, USA). Monoclonal anti-α_5 integrin Ig, monoclonal anti-α_2 integrin Ig, and monoclonal anti-β_1 integrin Ig, and the alkaline phosphatase-conjugated goat anti-mouse secondary antibodies, were purchased from Santa Cruz Biotechnology (Santa Cruz, CA, USA). All other chemicals were from Sigma-Aldrich and were of spectroscopic grade. Tissue culture flasks (75 cm^2) and 24-well tissue-culture plates were obtained from Laboratory Disposable Products (North Haledon, NJ, USA). Cells from a subclone of the MC3T3-E1 osteoblast-like cell line (subclone 4) that exhibit high levels of osteoblast differentiation (29), MG63 osteoblast-like cells, and the C3H10T1/2 mesenchymal stem cell line were obtained from the American Type Culture Collection (ATCC; Manassas, VA, USA). Cylindrical implant discs were initially prepared from Ti6Al4V sheets obtained from TIMET (Wentzville, MO, USA). The sheets were cut into strips, polished by machining, and then punched into discs (Industrial Tool & Die, Troy, NY, USA), as previously described (23).

Disk preparation

Highly polished Ti6Al4V discs were cleaned, passivated, treated in 40% nitric acid for 2 min, dried, sterilized, and stored. Some of the cleaned and passivated discs were treated with RFGD or heat (600 °C), as previously described (23), before sterilization. For heat treatment, discs were heated to a temperature of 600 °C in air for 1 h (23). Radiofrequency plasma glow discharge treatment of discs was performed using a modified Harrick RF unit (PDC- 002; Ossining, New York, NY, USA) with a quartz chamber to subject samples to an oxygen plasma treatment (23). The Ti6Al4V discs were passivated as previously described (21) to form a stable surface oxide layer and placed on a clean quartz tray. The tray was inserted into the RF unit and the unit was placed under dry vacuum (EcoDry-M oil-less vacuum pump; Leybold Vakuum, Koln, Germany). When the vacuum was low enough (1600 mTorr) to remove all water vapor, oxygen was gradually bled into the system via a needle valve. The gas flow rate was monitored using an Omega shielded flow meter (Omega Technologies, Stamford, CT, USA) at a rate of 250 ml/min. All oxygen gas was prefiltered before entry into the chamber (Advantec MFS, Pleasanton, CA, USA). Samples of titanium alloy were treated with a 13.56-MHz RF power-generated oxygen plasma for 5 min at 29.6 W (23). Following heat or RFGD treatment, discs were sterilized and stored as previously described for untreated specimens (21).

Surface analysis

Surfaces of untreated and treated discs were imaged by high-vacuum scanning electron microscopy (FEI, Quanta 600, Peabody, MA, USA) in the backscatter mode at 10,000X.

Measurements of HFN7.1 antibody binding to fibronectin

In order to monitor the capacity of surface pretreatments of Ti6Al4V to induce conformational changes in fibronectin that increase the exposure of its central integrin-binding domain, the binding of the HFN7.1 monoclonal antibody to adsorbed fibronectin was measured. The HFN7.1 antibody binds directly to the central integrin-binding domain

of fibronectin, is specific for human fibronectin, and does not cross-react with mouse or bovine fibronectin (30). Control and pretreated discs were placed in 96-well non-tissue-culture plates and then incubated with increasing concentrations of fibronectin (0.01 – 10 nM in PBS) overnight at room temperature in a sterile environment. The supernatant was aspirated, 200 μl of blocking buffer (0.25% BSA and 0.05% Tween-20 detergent) was added to each well, and the plate was incubated in a humid chamber for 2 h. The samples were washed with 1×PBS and distilled water, and incubated in 200 μl of a 1:25 dilution (in PBS) of an anti-fibronectin Ig (HFN7.1) for 1 h at 37°C. The samples were washed with PBS and distilled water, incubated in alkaline phosphatase-conjugated (goat anti-mouse) secondary antibody for 1 h at 37°C, and then washed again with PBS and distilled water. The samples were incubated in an alkaline phosphatase substrate (4-methyl umbelliferyl phosphate) for 2 h at room temperature and the relative fluorescence intensity (RFI; 365 nm excitation/450 nm emission) was measured in a TECAN Spectrofluorometer (Grodig, Austria). Data from four replicate discs for each fibronectin concentration for each of the experimental conditions were averaged to obtain the individual data points. Measurements of RFI for fibronectin-coated discs were corrected for RFI measured for uncoated discs.

Cell culture

MG63 (ATCC) cells were cultured in modified Eagle's medium + non-essential amino acids (MEM+NEAA) with heat-inactivated 10% FBS. MC3T3-E1 cells (subclone 4; ATCC) were cultured in MEM-α with 10% FBS. C3H10T1/2 mesenchymal stem cells (ATCC) were cultured in DME with 10% FBS.

Inhibitory effects of HFN7.1 antibody on osteogenic cell attachment

The proportion of attached osteogenic cells whose attachment was sensitive to inhibition by the HFN7.1 antibody was also measured to monitor changes in the exposure of the domain when adsorbed to pretreated surfaces. This proportion was measured as the percentage decrease in the number of attached cells observed when preadsorbed fibronectin was allowed to react with the HFN7.1 antibody before cells were introduced. The HFN7.1 antibody blocks the attachment of $\alpha_5\beta_1$ integrin to the central integrin-binding domain formed by the RGD and synergy sites by binding to an epitope located in a hinge region that joins the two sites (30). Whereas $\alpha_5\beta_1$ integrin mediates cell attachment to the central integrin-binding domain by binding to both the RGD and the synergy sites, $\alpha_v\beta_3$ integrin binds only to the RGD site (31). Therefore, because the HFN7.1 epitope lies outside the RGD-binding site (30), the HFN7.1 antibody will not inhibit cell attachment mediated by the binding of $\alpha_5\beta_1$,$\alpha_v\beta_3$,or other integrins to the RGD site alone in fibronectin (31). Any increase in the percentage blockade of cell attachment by the HFN7.1 antibody signifies an increase in the number of available central integrin-binding domain sites (as a proportion of the total cell-binding sites in fibronectin) or increased antibody binding to this domain. Enhanced availability of the central integrin-binding domain to $\alpha_5\beta_1$ integrins, or increased binding of the HFN7.1 antibody to this site, is presumably attributable to a greater conformational exposure. In order to test for non-specific effects of the HFN7.1 antibody on cell attachment that are caused by antibody binding outside the central integrin-binding domain of fibronectin, the anti-fibronectin Ig, IST-4, was used at the same range of concentrations as the HFN7.1 antibody as a negative control in these experiments. The IST-4 antibody does not bind to the central integrin-binding domain but instead recognizes an epitope located within the fifth type-III repeat of human fibronectin (Sigma-Aldrich product description). In contrast, the epitope in the central integrin-binding domain recognized by the HFN7.1 antibody is located in a "hinge" domain that spans the connection between the ninth and tenth type-III repeats of human fibronectin (30). Control discs or discs modified by heat (600 °C for 1 h) or RFGD (5 min) pretreatment were incubated with 10 nM fibronectin (in PBS, pH 7.4) in covered 96-well non-tissue-culture plates overnight at room

temperature under a cell-culture hood. The supernatant was then aspirated, 200 μl of 0.1% BSA/1× PBS was added to each well, and the liquid was aspirated 2 h later. MG63, MC3T3-E1, or C3H10T1/2 cells were then added to each well (150,000 cells/well) and incubated for 2 h at 37 °C. The samples were then washed six times with serum-free medium and the cell attachment number was quantified using a hexosaminidase assay (22). Cell attachment was corrected for the number of cells that attached in the absence of fibronectin coating. Cell attachment to fibronectin-coated untreated or treated discs was also measured in the presence of the monoclonal anti-fibronectin Ig, HFN7.1, at dilutions between 1:100 and 1:10 and a constant fibronectin-coating concentration of 10 nM, as previously described (22). The antibody was added to fibronectin-coated discs 10 min before the addition of cells. Data from multiple independent cell cultures for each antibody dilution and each surface category (untreated, heat-pretreated, or RFGD-pretreated) were averaged to obtain the individual data points.

Attachment of integrins to adsorbed fibronectin

$\alpha_5\beta_1$ integrin is the specific integrin receptor for fibronectin (32) and is the only major osteoblast integrin receptor that binds to the central integrin-binding domain of fibronectin (31). Therefore, the effects of Ti6Al4V pretreatment on the availability of the central integrin-binding domain for cell attachment were also assessed by measuring the binding of $\alpha_5\beta_1$ integrins to adsorbed fibronectin. The attachment of $\alpha_5\beta_1$ integrins to fibronectin was monitored by measuring the binding of anti-α_5 and anti-β_1 Igs to fibronectin–integrin receptor complexes by ELISA, as previously described (29). It is possible that any effects of our surface pretreatments on fibronectin binding to $\alpha_5\beta_1$ integrins could be attributable to increased generalized expression of multiple integrin subtypes. In order to test for this potential effect of the surface pretreatments, the binding of α_2 integrins to adsorbed fibronectin was measured because α_2 integrins do not bind to the central integrin-binding domain (31). An anti-α_2 integrin Ig was used at the same concentration as the as anti-α_5 integrin Ig (see later) as a negative control for experiments measuring the binding of $\alpha_5\beta_1$ integrins to adsorbed fibronectin. Control or pretreated discs in 96-well non-tissue-culture plates were coated with increasing concentrations of fibronectin (1, 10, 50, 100, and 500 nM in PBS) overnight at room temperature in a sterile environment. After removal of the coating solution, the samples were blocked in 1% heat-denatured BSA for 30 min. MC3T3 cells were detached from their flasks with trypsin-EDTA for 3 min and resuspended in serum-containing media. The cells were centrifuged, washed three times in PBS, and resuspended in DPBS containing 2 mM dextrose. MC3T3 cells were seeded onto substrates at 5,000–6,000 cells/mm^2 under serum-free conditions (2 mM dextrose in DPBS) for 1 h. Cell integrins were then chemically cross-linked to their bound ligand (adsorbed fibronectin) using the chemical cross-linker DTSSP; DTSSP is composed of two reactive sulfo-succinimide esters, one at each end of the molecule, which in combination are capable of forming covalent bonds with the primary amines of an integrin receptor and its bound ligand (fibronectin), thereby cross-linking the two proteins (33). Non-cross-linked cell-membrane proteins and cytosolic proteins were extracted using 0.1% SDS and 350 μg/ml of phenylmethylsulphonyl fluoride (PMSF) in cold DPBS (29). Cross-linked integrins were then probed with anti-α_5 (7.5 μg/ml), anti-α_2 (7.5 μg/ml) or anti-β_1 (1:100) integrin-specific primary antibodies. An alkaline phosphatase-conjugated secondary antibody (0.04 μg/ml) was then added in blocking buffer and allowed to react with the bound primary antibodies. Samples were then incubated with an alkaline phosphatase substrate (5-methyl umbelliferyl phosphate in diethanolamine buffer + 50 mM Na_2CO_3, pH 9.5; 60 μg/ml) for 45 min and fluorescence (365 nm excitation; 450 nm emission) was read in a TECAN Spectrofluorometer. Data from multiple independent cell cultures for each fibronectin concentration and each surface category (untreated, heat-pretreated, or RFGD-pretreated)

were averaged to obtain the individual data points. Measurements of RFI for fibronectin-coated discs were corrected for RFI measured for uncoated discs.

Statistical analysis

Data are presented as mean ± standard error of the mean. Statistical comparisons were performed using an ANOVA with the alpha level set at 0.05.

Results

Surface analysis

Scanning electron microscopy at 10,000× magnification showed that both the control discs and the treated discs exhibited significant topography, with peak-to-peak ranges of typically 200 nm in a 10 μm ×10 μm scan area. Virtually all this topography is caused by machining and polishing, resulting in parallel linear grooves with micron- and submicron-size features (Fig. 1). It was also observed that the RFGD treatment of Ti6Al4V discs did not alter the topography of the alloy surface (Fig. 1). Instead, the RFGD-treated surface looks at least as smooth as the control polished surface. In contrast, heat treatment altered oxide topography by creating a pattern of oxide elevations (Fig. 1). We have previously determined, by atomic force microscopy (AFM), that the oxide projections created by heat pretreatment were approximately 50–100 nm in diameter (23).

Effects of disc treatments on HFN7.1 antibody binding to adsorbed fibronectin

The HFN7.1 anti-fibronectin Ig recognizes an epitope in the central integrin-binding domain of fibronectin (30). We observed relatively low levels of binding of the HFN7.1 antibody to fibronectin adsorbed to untreated discs over a range of fibronectin-coating concentrations from 0.01 to 10 nM (Fig. 2). Significantly higher levels of antibody binding to fibronectin were detected for discs in the heat or RFGD pretreatment groups, with peak RFI levels of nearly 1,000 observed at 0.1 – 1 nM fibronectin. Notably, antibody binding appeared to reach a plateau for both untreated and treated discs at fibronectin-coating concentrations between 0.1 and 10 nM (Fig. 2).

Inhibition of osteogenic cell attachment to fibronectin-coated discs by the HFN7.1 antibody and effects of heat and RFGD pretreatments

The HFN7.1 antibody promoted a concentration-dependent inhibition of the attachment of MC3T3 (Fig. 3A) and MG63 (Fig. 3B) cells to adsorbed fibronectin. The antibody decreased the number of MC3T3 (Fig. 3A), MG63 (Fig. 3B), or C3H10T1/2 mesenchymal stem cells (unpublished results) that attached to fibronectin on untreated discs to 30 – 40% of the control (i.e. no antibody) levels. When tested at the same range of antibody dilutions that was employed for the HFN7.1 antibody, the IST-4 anti-fibronectin Ig failed to inhibit the attachment of MC3T3 cells to fibronectin adsorbed to untreated discs to any degree (Fig. 3A). In comparison with untreated discs, the HFN7.1 antibody decreased the number of cells that attached to fibronectin on heat or RFGD-pretreated discs to 0 – 20% of control levels (Fig. 3; and unpublished results with C3H10T1/2 cells). These results indicated that the RFGD and heat pretreatments of the alloy increased the percentage of attached MC3T3, MG63, and C3H10T1/2 cells whose attachment was sensitive to inhibition by the HFN7.1 antibody.

Effects of heat and RFGD pretreatments on the attachment of integrins to adsorbed fibronectin

The attachment of integrins to adsorbed fibronectin was measured by ELISA following chemical cross-linking of integrin receptor–fibronectin complexes (Fig. 4). For experiments

with fibronectin-coated untreated discs, the binding of anti-α_5 integrin Ig to integrin receptors that became attached to fibronectin progressively increased at higher concentrations of fibronectin (Fig. 5A). Notably, the levels of binding of the anti-α_5 integrin Ig were 10- to 20-fold higher for heat and RFGD-treated discs compared with untreated discs at fibronectin-coating concentrations of 1–10 nM (Fig. 5A). Antibody binding appeared to reach a plateau at a fibronectin-coating concentration of 10 – 500 nM for pretreated discs (Fig. 5A).

For untreated discs, the binding of an anti-β_1 integrin Ig to integrin receptors that attached to adsorbed fibronectin during cell incubation failed to increase as the fibronectin-coating concentration was increased from 1 to 100 nM (Fig. 5B). The heat and RFGD pretreatments increased the binding of the anti-β_1 integrin Ig compared with that of untreated discs at fibronectin-coating concentrations of 1 – 100 nM. The levels of anti-β_1 integrin Ig binding measured for RFGD-treated discs were 4- to 23-fold higher than those for untreated discs (Fig. 5B). However, only the heat pretreatment produced a statistically significant increase in the binding of the anti-β_1 integrin Ig compared with that of untreated discs at a fibronectin concentration of 100 nM (Fig. 5B). Neither heat nor RFGD pretreatments had any effect on the binding of the anti-α_2 integrin Ig to integrin receptors that attached to adsorbed fibronectin (Fig. 5C).

Discussion

We have previously reported that heat or RFGD surface pretreatments increase the attachment of osteogenic cells to adsorbed fibronectin without altering fibronectin's surface mass (22). In the current study, we began to investigate the biological mechanism responsible for the effects of heat or RFGD pretreatments of Ti6Al4V on the osteoblastic cell-attachment activity of fibronectin. We tested the hypothesis that these pretreatments modulate the intrinsic biological activity of fibronectin through inducing conformational changes that increase the exposure of the integrin-binding domain and its availability to form complexes with cell integrin receptors.

Our hypothesis was supported by results obtained from three types of experiments. In the first type of experiment, our findings demonstrated that heat and RFGD pretreatments increased the binding of the HFN7.1 antibody to adsorbed fibronectin. The HFN7.1 antibody binds specifically to the central integrin-binding domain of fibronectin (30), which contains a PHSRN synergy domain and an RGD site (34–36). In these experiments, measurements of antibody binding to fibronectin on coated discs were corrected for antibody binding to uncoated discs. Therefore, any non-specific effects of the treatments on background antibody binding to the uncoated discs were eliminated. We have previously shown that neither heat nor RFGD pretreatments increased the adsorption of fibronectin to Ti6Al4V when measured using an anti-fibronectin Ig directed against an epitope outside the central integrin-binding domain (22). This latter finding suggests that the pretreatments did not increase the number of binding sites for the HFN7.1 antibody by increasing the mass of adsorbed fibronectin. Instead, our findings in the current study suggest that surface pretreatments enhanced binding of the HFN7.1 antibody to fibronectin by increasing the exposure of the central integrin-binding domain.

In the second type of experiment performed in this study, we found that RFGD and heat pretreatments of the alloy increased the percentage of osteogenic cells whose attachment to fibronectin was sensitive to inhibition by the HFN7.1 antibody. This latter finding suggests that surface pretreatments increased the availability of the central integrin-binding domain of fibronectin for binding to cell integrins or the HFN7.1 antibody owing to greater conformational exposure of this site. It is possible that the HFN7.1 antibody disrupts cell

attachment to fibronectin by blocking other cell-binding sites outside the central integrin-binding domain or by promoting the complete unfolding of the molecule into a biologically inactive conformation. However, the failure of the anti-fibronectin Ig, IST-4, to inhibit osteogenic cell attachment to adsorbed fibronectin supports the specificity of the HFN7.1 antibody as a probe for measuring cell attachment that is directly mediated by the central integrin-binding domain. Notably, there is evidence that when this domain is blocked with soluble RGD peptides, a compensatory mechanism exists for the adhesion of osteoblasts to a fibronectin–tissue transglutaminase complex via syndecan-4, a transmembrane heparin sulphate proteoglycan receptor (37). Syndecan-4 also provides additional signalling for focal adhesion formation (38–39) by binding directly to fibronectin itself primarily via the HepII domain (containing the fibronectin type-III repeats 12–14) in the C-terminal region (40–42). In the current study, increases in the inhibition of the attachment of three different osteogenic cell lines to fibronectin to almost 100% on modified surfaces, mediated by the HFN7.1 antibody, suggests that pretreatments selectively increase attachment to the central integrin-binding domain. These findings also suggest that this domain represents the predominant osteoblast-adhesion site. Nevertheless, syndecan-4 binding may play some role in the observed cell attachment.

In the third type of experiment performed in this study, pretreatments also increased the binding of fibronectin to $\alpha_5\beta_1$ integrin, the specific receptor for the central integrin-binding domain (34–36). These findings provided further support for an enhancement in the availability of this site upon fibronectin adsorption to the modified surfaces. The observed increases in binding of the $\alpha_5\beta_1$ integrin are probably not attributable to a generalized increased expression of multiple integrin subtypes because the pretreatments failed to enhance the binding of α_2 integrins. The α_2 integrins are expressed in MC3T3 cells (43,44) but do not bind to the central integrin-binding domain (31). Therefore, our results collectively favour a mechanism in which the modified surface oxide induces conformational changes in fibronectin upon its adsorption that enhances the protein's intrinsic capacity to bind $\alpha_5\beta_1$ integrin receptors.

Our laboratory has investigated the influence of the physicochemical properties of oxide on the cell-attachment activity of adsorbed fibronectin (21–23). Using AFM, we previously showed that the heated surface exhibited RMS roughness values (12.8 ± 1.7 nm) that were three-fold higher than those of untreated (4.1 ± 1.1 nm) or RFGD-treated (3.6 ± 0.9 nm) discs (23). In the current study, scanning electron microscopy analyses confirmed our previous findings that only heat treatment altered Ti6Al4V surface-oxide roughness and topography (35). We previously analyzed the effects of heat and RFGD on the net charge of the oxide using AFM. In these latter experiments, the electrostatic forces between the oxide surface and a negatively charged silicon nitride probe were used to estimate the net charge of the oxide (23). Force spectroscopy measurements demonstrated that both the RFGD and heat pretreatments made the surface oxide of Ti6Al4V more negatively charged at physiological pH (23). In a related study, we demonstrated that the stimulatory effects of heat and RFGD treatments on the cell-attachment activity of adsorbed fibronectin were more highly correlated with an increase in the negative net charge of the oxide than with other oxide characteristics (22). In the current study, we showed that the stimulatory effects of both treatments on the conformational bioactivity of the central integrin-binding domain of fibronectin were also more highly correlated with oxide charge than with oxide topography or roughness.

Local metal oxide charge can be influenced by the acid–base balance of metal hydroxo-complexes (45). The hydroxo-complexes of multivalent metal cations are amphoteric, exhibiting both acidic and basic properties:

$$M - OH + H_2O \rightarrow [M - O]^- + H_3O^+ \text{ (acidic reaction)}$$
$$M - OH + H_2O \rightarrow [M - OH_2]^+ + OH^- \text{ (basic reaction)}$$

Each metal is likely to have a unique isoelectric point, the pH at which there is an equal proportion of $[M–O]^-$ and $[M–OH2]^+$ groups, and there are no uncompensated charges. The effects of the pretreatments on the net negative charge of the oxide at physiological pH are likely to have arisen from an elevation in the surface concentration of uncompensated negative charges from $[M\text{-}O]^-$ groups. During the process of fibronectin adsorption to the alloy, $[M\text{-}O]^-$ species that are free to bind to the protein can theoretically form bonds with positively charged basic amino-acid residues, potentially disrupting bonds within the protein and destabilizing its conformation. Our findings that the pretreatments increase oxide negative charge (23), cell attachment to adsorbed fibronectin (22), and the availability of the integrin-binding domain, as reported here, suggest that $[M\text{-}O]^-$ groups have the potential to modulate the conformation and bioactivity of fibronectin.

It has been demonstrated that negatively charged substrates can disrupt intermolecular interactions between the two cross-linked polypeptide chains of the fibronectin homodimeric protein to form a more relaxed or elongated conformation of the dimeric protein (24–26). Similarly, the electrostatic effects of negatively charged functionalities in a substrate may also disrupt intramolecular associations within individual fibronectin monomers, resulting in localized conformational changes in specific molecular domains. The sensitivity of any particular peptide region to the effects of substrate charge on the three-dimensional protein structure may also be influenced by the presence of charged amino acids. Using silica as a substrate, it has been shown that interactions involving $Si\text{-}O^-$ groups occur mainly with e-amino groups of basic lysine residues, guanidine moieties of basic arginine residues, and N-terminal amino groups (46). Interactions between a negatively charged COOH-functionalized substrate (consisting of pyridinyl-terminated self-assembled alkanethiol monolayers) and positively charged lysines have been reported to induce conformational changes in cytochrome *c* when bound to the substrate (47). Another study demonstrated that the chemical modification of lysines caused extensive conformational changes in fibronectin in solution (48). This latter finding suggests that charged substrates might promote conformational changes in fibronectin by disrupting intramolecular associations involving positively charged amino acids such as lysines. Notably, it has also been shown that binding of the HFN7.1 antibody to fibronectin, fibronectin binding to $\alpha_5\beta_1$ integrins, and cell adhesion strength were all higher for OH-functionalized self-assembled alkanethiol monolayers compared with positively charged or hydrophobic surfaces (49). These findings collectively suggest that the binding of cationic basic amino acids in fibronectin to anionic $M\text{-}O^-$ groups in the oxide of Ti6Al4V can similarly disrupt intramolecular electrostatic interactions in the integrin-binding domain, thereby altering its conformation and bioactivity.

Fibronectin contains a number of binding sites, including those for collagen and heparin, as well as an RGD domain that integrins recognize as an important cell-binding site (20). The binding of $\alpha_5\beta_1$ integrin to fibronectin requires both the PHSRN synergy domain in the ninth type-III repeat and the RGD motif in the tenth type-III repeat of the molecule, collectively referred to as the central integrin-binding domain (34). X-ray crystallographic data suggests that the PHSRN synergy and RGD sites are exposed on the same face of the molecule (50). However, the energetics of adsorption to a substrate may influence the rotation or extension of the bonds joining these repeats, thereby changing the distance between the RGD and the synergy domains. Increases in the spacing between the synergy domain and the RGD domain prevented the binding of fibronectin (coated on polystyrene) to

$\alpha_5\beta_1$ integrins in kidney cells and stromal fibroblasts and the downstream cell-adhesion events of spreading and phosphorylation of focal adhesion kinase (51). The HFN7.1 antibody employed in our study recognizes an epitope that is mapped to residues 1359–1436 and located in a "hinge" domain that spans the connection between the ninth and tenth type-III repeats and lies outside the RGD-binding site (30). Therefore, it is likely that conformational changes in the hinge region that joins the RGD and synergy sites to create the central integrin-binding domain would influence the binding of this domain to both $\alpha_5\beta_1$ integrins and the HFN7.1 antibody. Notably, both heat and RFGD pretreatments increased the binding of $\alpha_5\beta_1$ integrins and the HFN7.1 antibody to adsorbed fibronectin. These results suggest that an enhancement in negatively charged oxides, created by our surface pretreatments at physiological pH (23), induced conformational changes in the hinge region of fibronectin that increased the exposure of the central integrin-binding domain. It is further proposed that the altered charge properties of the oxide may induce a selective unfolding of the hinge region, thereby creating a physical space between the RGD and synergy sites that favours binding to $\alpha_5\beta_1$ integrins.

In summary, our results suggest that negatively charged functionalities in the Ti6Al4V surface oxide induce conformational changes in fibronectin upon adsorption that increase the availability of the integrin-binding domain to $\alpha_5\beta_1$ integrins. These results help to explain our previous findings that more osteogenic cells attach to fibronectin when preadsorbed to a highly charged surface oxide compared with an oxide of lower surface charge. (22). The current study demonstrates how the physico-chemical properties of the Ti6Al4V surface oxide may be modified to alter the three-dimensional structure and bioactivity of fibronectin when used as an implant surface coating. A better understanding of surface-modulated protein conformation and related cellular behaviour is essential for the design of optimally bioactive implant surfaces that may be useful in improving implant longevity. Future studies will further investigate the relationship between metal oxide properties and protein structure and activity.

Acknowledgments

The project described was supported by Grant Number NIH RO1 DE017695 (awarded to D.E.M.). This material is also the result of work supported with resources and the use of facilities at the James J. Peters VA Medical Center, Bronx, New York. This investigation was also conducted at the HSS research facility constructed with support of Grant C06-RR12538–01 from the National Center for Research Resources, NIH. We would like to acknowledge Dr Stephen Doty and Tony Labisserie for their help with scanning electron microscopy. Special thanks go to Tiffany Leung, Ryan Jeong, and Kyle Hackshaw for their technical assistance.

References

1. WEBSTER TJ. Improved bone tissue engineering materials. Am Ceram Soc Bull. 2003; 82:23–28.
2. ADELL R, ERIKSEN B, LEKHOLM U, BRANEMARK PI, JEMT T. A long-term follow-up study of osseointegrated implants in the treatment of totally edentulous jaws. Int J Oral Maxillofac Implants. 1990; 5:347–359. [PubMed: 2094653]
3. ADELL R, LEKHOLM U, ROCKLER B, BRANEMARK PI. A 15-year study of osseointegrated implants in the treatment of the edentulous jaw. Int J Oral Surg. 1981; 10:387–416. [PubMed: 6809663]
4. HARDT CR, GRONDAHL K, LEKHOLM U, WENNSTROM JL. Outcome of implant therapy in relation to experienced loss of periodontal bone support: A retrospective 5-year study. Clin Oral Implants Res. 2002; 13:488–94. [PubMed: 12453125]
5. FRIBERG B, SENNERBY L, ROOS J, JOHANSSON P, STRID KG, LEKHOLM U. Evaluation of bone density using cutting resistance measurements and microradiography:an in vitro study in pig ribs. Clin Oral Implants Res. 1995; 6:164–71. [PubMed: 7578792]
6. WILLIAMS DF. Implants in dental and maxillofacial surgery. Biomaterials. 1981; 2:133–146. [PubMed: 7023554]

7. IMAM, MA.; FRAKER, AC. Titanium alloys as implant materials. In: BROWN, SA.; LEMONS, JE., editors. Medical applications of titanium and its alloys. Philadelphia: American Society for Testing and Materials; 1996. p. 3-16.
8. MORRIS HF, WINKLER S, OCHI S. A 48-month multicenter clinical investigation: implant design and survival. J Oral Implantol. 2001; 27:180–186. [PubMed: 12500876]
9. KASEMO B. Biocompatibility of titanium implants:surface science aspects. J Prosthetic Dent. 1983; 49:832–837.
10. SOUSA SR, LAMGHARI M, SAMPAIO P, MORADAS-FERREIRA P, BARBOSA MA. Osteoblast adhesion and morphology on TiO2 depends on the competitive preadsorption of albumin and fibronectin. J Biomed Mater Res A. 2008; 84:281–290. [PubMed: 17607748]
11. GARCIA A, REYES C. Bio-adhesive surfaces to promote osteoblast differentiation and bone formation. J Dent Res. 2005; 84:407–413. [PubMed: 15840774]
12. SIEVING A, WU B, MAYTON L, NASSER S, WOOLEY PH. Morphological characteristics of total joint arthroplasty-derived ultra-high molecular weight polyethylene (UHMWPE) wear debris that provoke inflammation in a murine model of inflammation. J Biomed Mater Res. 2003; 64A: 457–464.
13. RAPUANO BE, WU C, MACDONALD DE. Osteoblast-like cell adhesion to bone sialoprotein peptides. J Orthop Res. 2004; 22:353–361. [PubMed: 15013096]
14. SAUBERLICH S, KLEE D, RICHTER EJ, HOCKER H, SPIEKERMANN H. Cell culture tests for assessing the tolerance of soft tissue to variously modified titanium surfaces. Clin Oral Implants Res. 1999; 10:379–393. [PubMed: 10551063]
15. MACDONALD DE, DEO N, MARKOVIC B, STRANICK M, SOMASUNDARAN P. Adsorption and dissolution behavior of human plasma fibronectin on thermally and chemically modified titanium dioxide particles. Biomaterials. 2002; 23:1269–1279. [PubMed: 11791930]
16. MACDONALD DE, MARKOVIC B, ALLEN M, SOMASUNDARAN P, BOSKEY AL. Surface analysis of human plasma fibronectin adsorbed to commercially pure titanium materials. J Biomed Materials Res. 1998; 41:120–130.
17. HARBERS GM, HEALY KE. The effect of ligand type and density on osteoblast adhesion, proliferation, and matrix mineralization. J Biomed Mater Res. 2005; 75:855–869.
18. BARBER TA, GOLLEDGE SI, CASTNER DG, HEALY KE. Peptide-modified p(AAm-co-EG/AAc) IPN's grafted to bulk titanium modulate osteoblast behavior *in vitro*. J Biomed Mater Res. 2003; 64:38–47.
19. REZANIA A, THOMAS CH, BRANGER AB, WATERS CM, HEALY KE. The detachment strength and morphology of bone cells contacting materials modified with a peptide sequence found within bone sialoprotein. J Biomed Mater Res. 1997; 37:9–19. [PubMed: 9335344]
20. HYNES RO. Integrins : bidirectional, allosteric signaling machines. Cell. 2002; 110:673–687. [PubMed: 12297042]
21. MACDONALD DE, RAPUANO BE, DEO N, STRANICK M, SOMASUNDARAN P, BOSKEY AL. Thermal and chemical modification of titanium-aluminum-vanadium implant materials: effects on surface properties, glycoprotein adsorption, and MG63 cell attachment. Biomaterials. 2004; 25:3135–3146. [PubMed: 14980408]
22. RAPUANO BE, MACDONALD DE. Surface oxide net charge of a titanium alloy : Modulation of fibronectin-activated attachment and spreading of osteogenic cells. Colloids and Surface B : Biointerfaces. 2011; 82:95–103.
23. MACDONALD DE, RAPUANO BE, SCHNIEPP HC. Surface oxide net charge of a titanium alloy : comparison between effects of treatment with heat or radiofrequency plasma glow discharge. Colloids and Surface B : Biointerfaces. 2011; 82:173–181.
24. BERGKVIST M, CARLSSON J, OSCARSSON S. Surface-dependent conformations of human plasma fibronectin adsorbed to silica, mica, and hydrophobic surfaces, studied with use of atomic force microscopy. J Biomed Mater Res. 2003; 64A:349–356.
25. BAUGH L, VOGEL V. Structural changes of fibronectin adsorbed to model surfaces probed by fluorescence resonance energy transfer. J Biomed Mater Res. 2004; 69A:525–534.
26. KOWALCZYNSKA HM, KOLOS R, NOWAK-WYRZYKOWSKA M, DOBKOWSKI J, ELBAUM D, SZCZEPANKIEWICZ A, KAMIN J. Atomic force microscopy evidence for

conformational changes of fibronectin adsorbed on unmodified and sulfonated polystyrene surfaces. J Biomed Mater Res. 2009; 91A:1239–1251.

27. MILLER T, BOETTIGER D. Control of intracellular signaling by modulation of fibronectin conformation at the cell-materials interface. Langmuir. 2003; 19:1723–1729.
28. LEE MH, DUCHEYNE P, LYNCH L, BOETTIGER D, COMPOSTO RJ. Effect of biomaterial surface properties on fibronectin-$\alpha_5\beta_1$ integrin interaction and cellular attachment. Biomaterials. 2006; 27:1907–1916. [PubMed: 16310247]
29. KESELOWSKY BG, GARCIA AJ. Quantitative methods for analysis of integrin binding and focal adhesion formation on biomaterial surfaces. Biomaterials. 2005; 26:413–418. [PubMed: 15275815]
30. BOWDITCH RD, HALLORAN CE, AOTA S, OBARA M, PLOW EF, YAMADA KM, GINSBERG MH. Integrin alpha IIb beta 3 (platelet GPIIb-IIIa) recognizes multiple sites in fibronectin. J Biol Chem. 1991; 266:23323–23328. [PubMed: 1720779]
31. DANEN EH, AOTA S, VAN KRAATS AA, YAMADA KM, RUITER DJ, VAN MUNJEN GN. Requirement for the synergy site for cell adhesion to fibronectin depends on the activation state of integrin alpha 5 beta 1. J Biol Chem. 1995; 270:21612–21618. [PubMed: 7545166]
32. ARGRAVES WS, SUZUKI S, ARAI H, THOMPSON K, PIERSCHBACHER MD, RUOSLAHTI E. Amino acid sequence of the human fibronectin receptor. J Cell Biol. 1987; 105:1183–1190. [PubMed: 2958481]
33. BENNETT KL, KUSSMAN M, BJORK P, GODZWON M, MIKKELSEN M, SORENSEN P, ROEPSTORFF P. Chemical cross-linking with thiol-cleavable reagents combined with different mass spectrometric peptide mapping – A novel approach to assess intermolecular protein contacts. Protein Sci. 2000; 9:1503–1518. [PubMed: 10975572]
34. AOTA S, NOMIZU M, YAMADA KM. The short amino acid sequence Pro-His-Ser-Arg-Asn in human fibronectin enhances cell-adhesive function. J Biol Chem. 1994; 269:24756–24761. [PubMed: 7929152]
35. REDICK SD, SETTLES DL, BRISCOE G, ERICKSON HP. Defining fibronectin's cell adhesion synergy site by site-directed mutagenesis. J Cell Biol. 2000; 149:521–527. [PubMed: 10769040]
36. GARCIA AJ, SCHWARZBAUER JE, BOETTIGER D. Distinct activation states of $\alpha_5\beta_1$ integrin show differential binding to RGD and synergy domains of fibronectin. Biochem. 2002; 41:9063–9069. [PubMed: 12119020]
37. WANG Z, TELCI D, GRIFFIN M. Importance of syndecan-4 and syndecan -2 in osteoblast cell adhesion and survival mediated by a tissue transglutaminase-fibronectin complex. Exp Cell Res. 2011; 317:367–381. [PubMed: 21036168]
38. WOODS A, COUCHMAN JR, JOHANSSON S, HOOK M. Adhesion and cytoskeletal organization of fibroblasts in response to fibronectin fragments. EMBO J. 1986; 5:665–670. [PubMed: 3709521]
39. BLOOM L, INGHAM KC, HYNES RO. Fibronectin regulates assembly of actin filaments and focal contacts in cultured cells via the heparin-binding site in repeat III13. Mol Biol Cell. 1999; 10:1521–1536. [PubMed: 10233160]
40. BASS MD, HUMPHRIES MJ. Cytoplasmic interactions of syndecan-4 orchestrate adhesion receptor and growth factor receptor signaling. Biochem J. 2002; 368:1–15. [PubMed: 12241528]
41. COUCHMAN JR. Syndecans : proteoglycan regulators of cell surface microdomains? Nat Rev Mol Cell Biol. 2003; 4:926–937. [PubMed: 14685171]
42. INGHAM KC, BREW SA, ATHA DH. Interaction of heparin with fibronectin and isolated fibronectin domains. Biochem J. 1990; 272:605–611. [PubMed: 2268289]
43. PARK JW, KIM YJ, JANG JH, SONG H. Osteoblast response to magnesium ion-incorporated nanoporous titanium oxide sufaces. Clin Oral Implants Res. 2011; 21:1278–1587. [PubMed: 20497442]
44. YANG RS, LIN WL, CHEN YZ, TANG CH, HUANG TH, LU BY, FU WM. Regulation by ultrasound treatment on the integrin expression and differentiation of osteoblasts. Bone. 2005; 36:276–283. [PubMed: 15780953]
45. VARGO TG, BEKOS EJ, KIM YS, RANIERI JP, BELLAMKONDA R, AEBISCHER P, MARGEVICH DE, THOMPSON PM, BRIGHT FV, GARDELLA JA JR. Synthesis and

characterization of fluoropolymeric substrata with immobilized minimal peptide sequences for cell adhesion studies. I J Biomed Mater Res. 1995; 29:767–778.

46. HAMRNIKOVA I, MIKSIK I, DEYL Z, KASICKA V. Binding of proline and hydroxyprolin-containing peptides to the capillary wall. J Chromatogr. 1999; 838:167–177.
47. MURGIDA DH, HILDEBRANDT P. Surface-enhanced resonance raman spectroscopic and electrochemical study of cytochrome *c* bound on electrodes through coordination with pyridinyl-terminated self-assembled monolayers. J Phys Chem. 2004; 108:2261–2269.
48. VUENTO M, STENMAN U-H, SALONEN E, OSTERLUND K, KUUSELAS P. Effect of chemical modification of arginine and lysine residues of fibronectin on its antigenic and gelatin-binding activity. Molec Immunol. 1983; 20:149–153. [PubMed: 6405197]
49. KESELOWSKY BG, COLLARD DM, GARCIA AJ. Surface chemistry modulates fibronectin conformation and directs integrin binding and specificity to control cell adhesion. J Biomed Mater Res. 2003; 66A:247–259.
50. LEAHY DJ, AUKHIL I, ERICKSON HP. 2. 0 A crystal structure of a four-domain segment of human fibronectin encompassing the RGD loop and synergy region. Cell. 1996; 84:155–164. [PubMed: 8548820]
51. GRANT RP, SPITZFADEN C, ALTROFF H, CAMPBELL ID, MARDON HJ. Structural requirements for biological activity of the ninth and tenth FIII domains of human fibronectin. J Biol Chem. 1997; 272:6159–6166. [PubMed: 9045628]

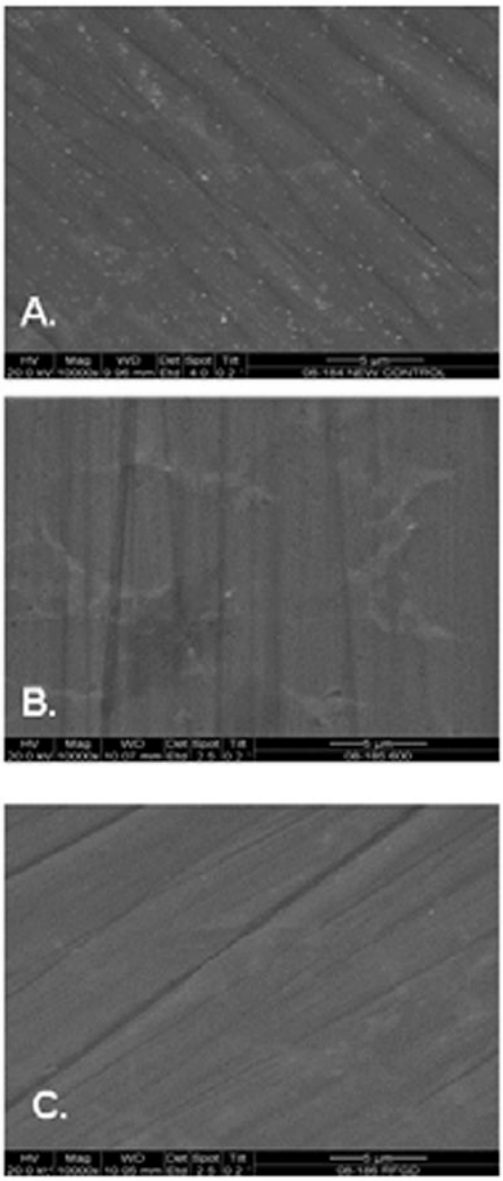

Figure 1.
Effects of heat and radiofrequency plasma glow discharge (RFGD) treatment on the surface finish of titanium alloy (Ti6Al4V) discs. Disks were polished then (A) untreated, (B) heat-treated, or (C) RFGD-treated and imaged at 10,000X magnification by scanning electron microscopy.

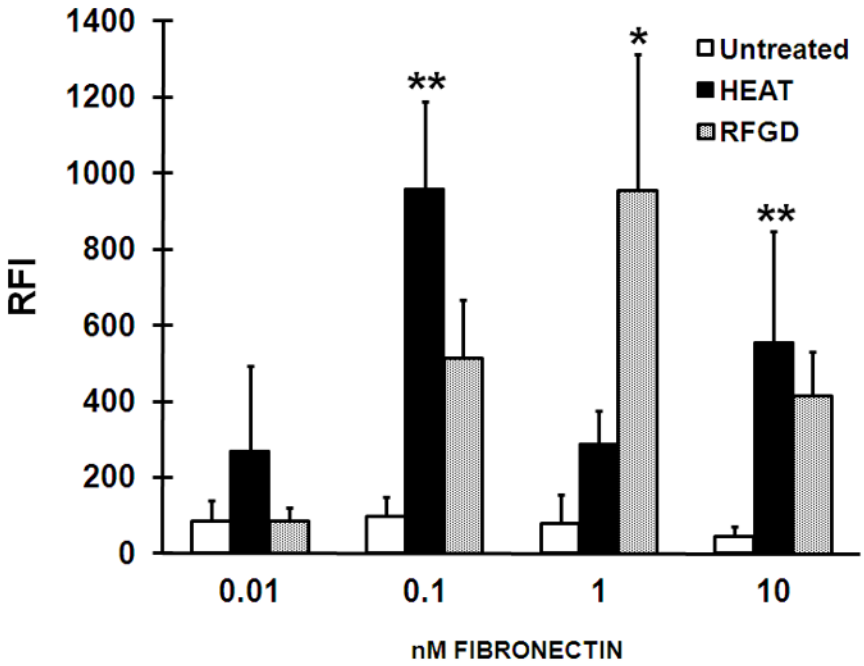

Figure 2.

Effects of heat and radiofrequency plasma glow discharge (RFGD) treatments on the binding of the HFN7.1 antibody to adsorbed fibronectin. Untreated: passivated untreated titanium alloy (Ti6Al4V) discs were left uncoated or were precoated overnight with the indicated concentrations of fibronectin. HEAT and RFGD: passivated discs were pretreated with heat or RFGD, respectively, and then left uncoated or precoated overnight with the indicated concentrations of fibronectin. Following the coating period, the discs were incubated with the HFN7.1 anti-fibronectin Ig and a fluorometric ELISA was performed to quantify the binding of the antibody to fibronectin. The relative fluorescence intensity (RFI) measurements obtained at each coating concentration of fibronectin (1 nM corresponds to 0.44 μg/ml of fibronectin) are presented. Measurements of RFI for fibronectin-coated discs were corrected for RFI measured for uncoated discs. Data from four replicate discs for each fibronectin concentration and for each of the experimental conditions were averaged to obtain the individual data points shown. Data represent mean ± SE. * > untreated group at the corresponding coating concentration of fibronectin ($p < 0.01$); ** > untreated group at the corresponding coating concentration of fibronectin ($p < 0.001$) based on ANOVA.

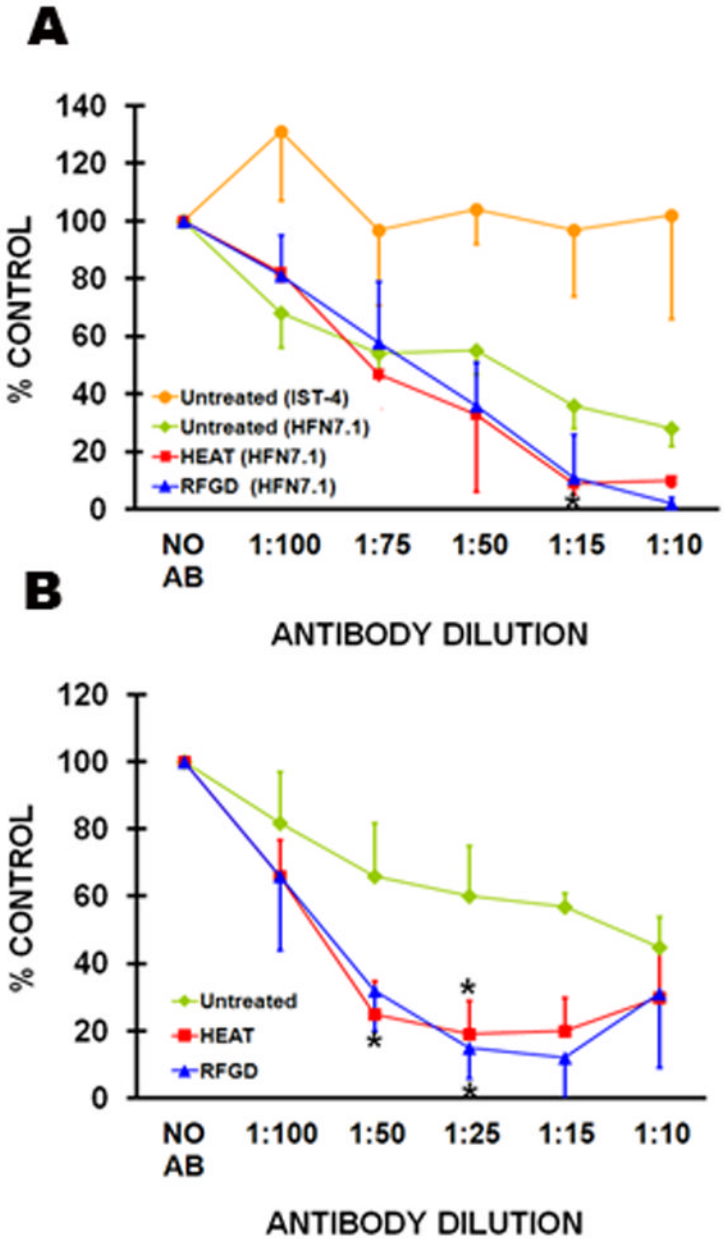

Figure 3.

Inhibition of attachment of MC3T3 cells to fibronectin-coated discs by the HFN7.1 antibody and the effect of pretreatment with heat (HEAT) and with radiofrequency plasma glow discharge (RFGD). Untreated and pretreated discs were coated overnight with 1 nM (0.44 μg/ml) fibronectin, incubated with cells for 2 h, and the number of (A) MC3T3 or (B) MG63 cells that attached to coated discs was measured in the presence of various dilutions of the HFN7.1 anti-fibronectin Ig. The number of cells that attached to these discs at each antibody dilution was measured, corrected for background cell attachment, and then expressed as a percentage of the attached cell number (corrected for background) measured for coated discs in the absence of antibody. The background cell attachment is the number of cells that attached in the absence of both the antibody and the fibronectin coating. In experiments using the HFN7.1 antibody, data for untreated discs were obtained from four to

six independent cell cultures for each antibody dilution, data for HEAT-pretreated discs were obtained from six independent cell cultures, and data for RFGD-pretreated discs were obtained from three to four independent cell cultures. Data from three independent cultures of MC3T3 cells are also presented for the IST-4 anti-fibronectin Ig that was tested as a negative control for experiments using untreated discs only. AB, antibody. Data represent mean ± SE. * > untreated group at the corresponding antibody dilution ($p < 0.05$) based on ANOVA.

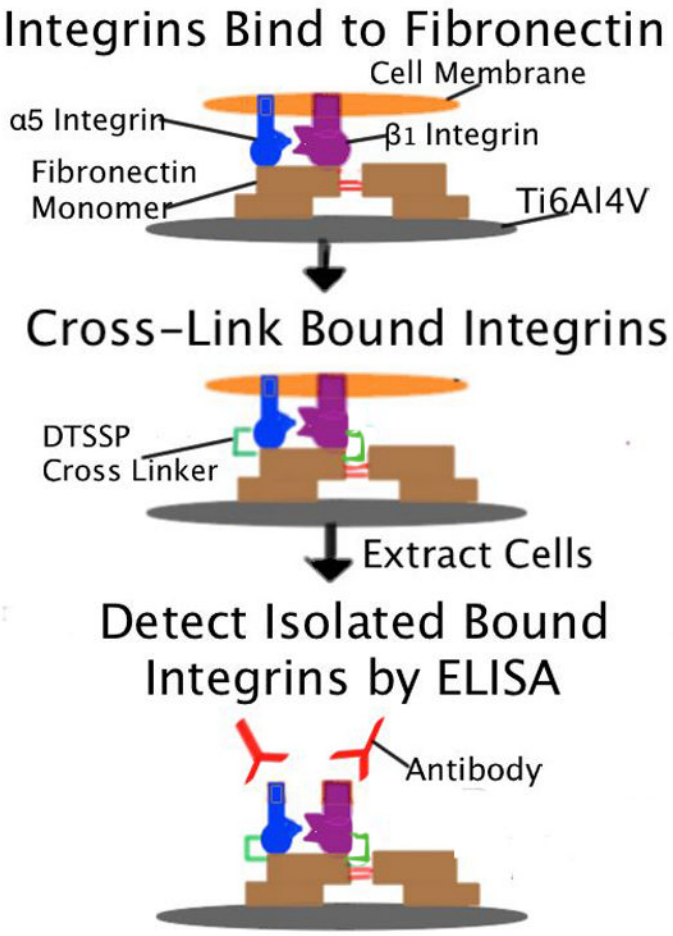

Figure 4.

Procedure for measuring the binding of anti-integrin Igs to integrin receptors that became attached to adsorbed fibronectin during incubation with MC3T3 cells. Untreated and pretreated discs were coated overnight with various concentrations of fibronectin and incubated with MC3T3 cells for 2 h. After integrins were cross-linked to their bound ligand (adsorbed fibronectin), non-cross-linked cell proteins were extracted and the binding of anti-integrin Igs to cross-linked integrins was quantified by ELISA, as depicted schematically for the $\alpha_5\beta_1$ integrin receptor.

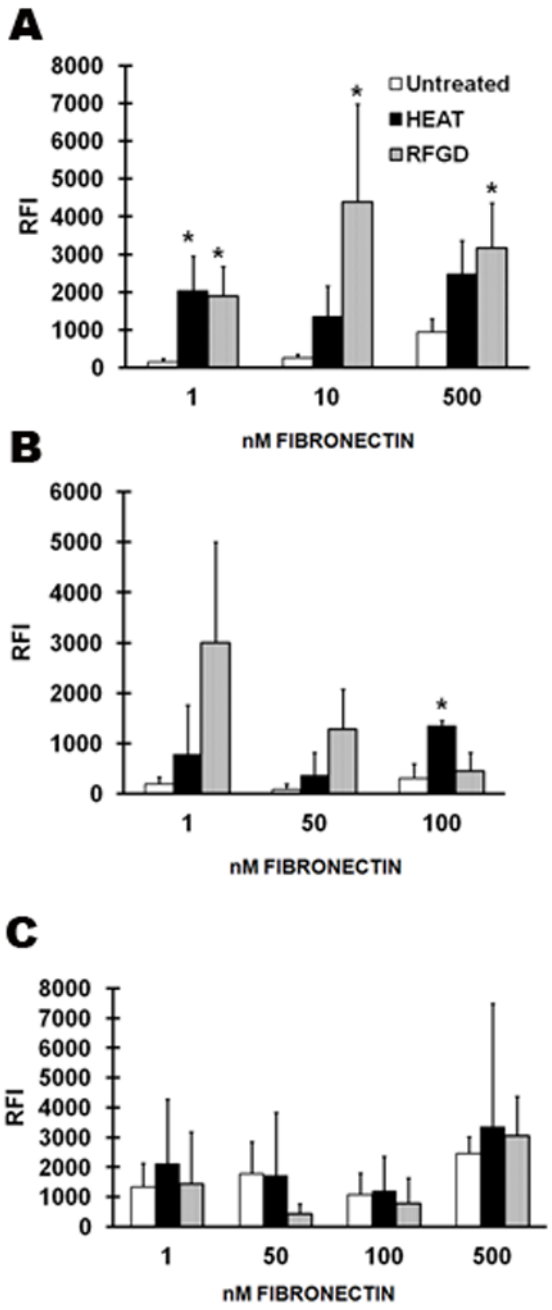

Figure 5.

Effects of pretreatment with heat and with radiofrequency plasma glow discharge (RFGD) on the binding of anti-integrin Igs to integrin receptors that became attached to adsorbed fibronectin during incubation with MC3T3 cells. Untreated and pretreated discs were coated overnight with various concentrations of fibronectin and then incubated with MC3T3 cells for 2 h. The binding of (A) an anti-α_5 integrin Ig, (B) an anti-β_1 integrin Ig, or (C) an anti-α_2 integrin Ig to cross-linked integrins was quantified as shown in Figure 4. The relative fluorescence intensity (RFI) measurements obtained at each indicated coating concentration of fibronectin (1 nM corresponds to 0.44 μg/ml of fibronectin) are presented. Data for untreated discs were obtained from three to six independent cell cultures for each antibody

dilution and data for heat-pretreated and RFGD-pretreated discs were obtained from three independent cell cultures. Data represent mean ± SE. * > untreated group at the corresponding fibronectin-coating concentration ($p < 0.05$) based on ANOVA.